JACS
JOURNAL OF THE AMERICAN CHEMICAL SOCIETY
Article
pubs.acs.org/JACS

Mechanism of the $AppA_{BLUF}$ Photocycle Probed by Site-Specific Incorporation of Fluorotyrosine Residues: Effect of the Y21 pK_a on the Forward and Reverse Ground-State Reactions

Agnieszka A. Gil,[†,#] Allison Haigney,[†,#] Sergey P. Laptenok,[‖] Richard Brust,[†] Andras Lukacs,[¶] James N. Iuliano,[†] Jessica Jeng,[†] Eduard H. Melief,[†] Rui-Kun Zhao,[‖] EunBin Yoon,[†] Ian P. Clark,[⊥] Michael Towrie,[⊥] Gregory M. Greetham,[⊥] Annabelle Ng,[§] James J. Truglio,[§] Jarrod B. French,[†,‡] Stephen R. Meech,[*,‖] and Peter J. Tonge[*,†]

[†]Department of Chemistry, and [‡]Department of Biochemistry & Cell Biology, Stony Brook University, Stony Brook, New York 11794-3400, United States

[§]William A. Shine Great Neck South High School, 341 Lakeville Road, Great Neck, New York 11020, United States

[¶]Department of Biophysics, Medical School, Szigeti Strasse 12, H-7624 Pécs, Hungary

[‖]School of Chemistry, University of East Anglia, Norwich Research Park, Norwich NR4 7TJ, United Kingdom

[⊥]Central Laser Facility, Harwell Science and Innovation Campus, Didcot, Oxon OX11 0QX, United Kingdom

Supporting Information

ABSTRACT: The transcriptional antirepressor AppA is a blue light using flavin (BLUF) photoreceptor that releases the transcriptional repressor PpsR upon photoexcitation. Light activation of AppA involves changes in a hydrogen-bonding network that surrounds the flavin chromophore on the nanosecond time scale, while the dark state of AppA is then recovered in a light-independent reaction with a dramatically longer half-life of 15 min. Residue Y21, a component of the hydrogen-bonding network, is known to be essential for photoactivity. Here, we directly explore the effect of the Y21 pK_a on dark state recovery by replacing Y21 with fluorotyrosine analogues that increase the acidity of Y21 by 3.5 pH units. Ultrafast transient infrared measurements confirm that the structure of AppA is unperturbed by fluorotyrosine substitution, and that there is a small (3-fold) change in the photokinetics of the forward reaction over the fluorotyrosine series. However, reduction of 3.5 pH units in the pK_a of Y21 increases the rate of dark state recovery by 4000-fold with a Brønsted coefficient of ∼1, indicating that the Y21 proton is completely transferred in the transition state leading from light to dark adapted AppA. A large solvent isotope effect of ∼6−8 is also observed on the rate of dark state recovery. These data establish that the acidity of Y21 is a crucial factor for stabilizing the light activated form of the protein, and have been used to propose a model for dark state recovery that will ultimately prove useful for tuning the properties of BLUF photosensors for optogenetic applications.

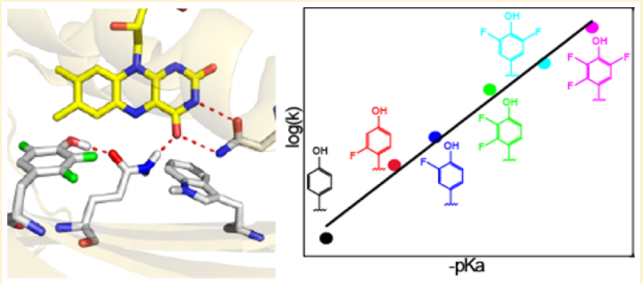

INTRODUCTION

The blue light using FAD (BLUF) domain proteins are a class of photoreceptors that utilize a noncovalently bound flavin to sense and respond to light.[1] BLUF domains are found in many species where they regulate the light-dependent activity of a variety of biological processes through an output domain that is either fused to the BLUF domain or forms a noncovalent complex with it.[1−5] The BLUF signaling state is formed on the nanosecond time scale and is characterized by a 10−15 nm red shift in the absorption spectrum of the flavin. Once formed, the photoactivated state returns to the dark state in a light-independent reaction that occurs in seconds to minutes, depending on the BLUF domain. There is significant interest in understanding how light absorption leads to photoreceptor activation, partly because in AppA the flavin chromophore, unlike other photosensors, is unable to undergo large-scale structural changes upon photoexcitation, but also more broadly because the BLUF domain proteins represent a model for determining how variations in light intensity lead to the control of gene expression in living organisms.

AppA is the best characterized BLUF domain photoreceptor and is found in *Rhodobacter sphaeroides* where it acts as an antirepressor of photosystem biosynthesis. In the dark AppA binds PpsR, a transcription factor, forming an AppA-$PpsR_2$ complex. When irradiated with blue light, the complex dissociates releasing PpsR, enabling it to bind to DNA and repress photosystem biosynthesis.[1] Absorption of light leads to

Received: October 23, 2015
Published: December 26, 2015

DOI: 10.1021/jacs.5b11115
J. Am. Chem. Soc. 2016, 138, 926−935

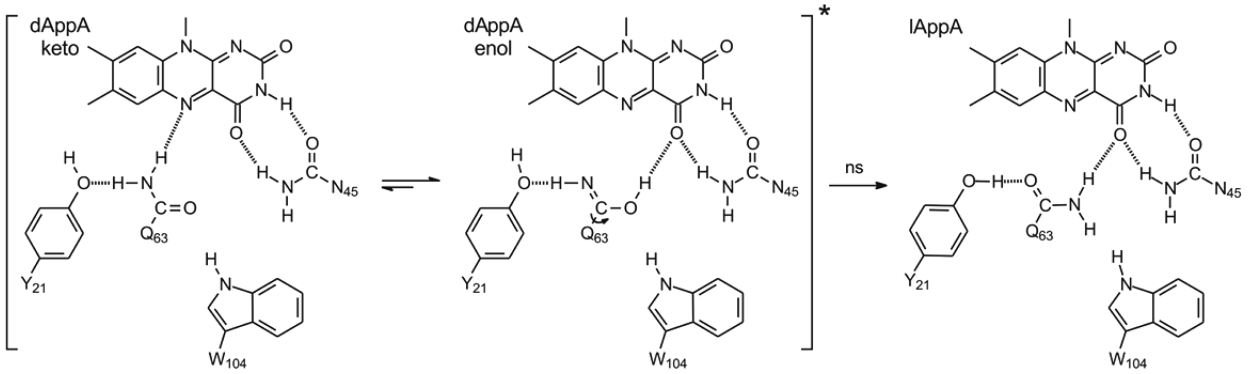

Figure 1. Mechanism of AppA light state formation. Flavin chromophore is surrounded by a hydrogen-bonding network that includes Y21, Q63, and W104. W104 is shown close to the hydrogen-bonding network in both the dark and the light states; however, the position of this residue in both states remains to be fully elucidated. Photoactivation of dark adapted AppA (dAppA) is proposed to proceed via keto−enol tautomerism of Q63 resulting ultimately in rotation of Q63 in the light state (lAppA).[9,16] Hydrogen bonds are shown as dashed lines, and formation of lAppA results in an additional hydrogen bond with the flavin C4═O.

an ultrafast rearrangement of a hydrogen-bonding network which ultimately leads to the signaling state of the protein.[5,6] However, the mechanism leading to these structural changes and how they relate to BLUF domain activity remain to be fully elucidated.[7−9]

The hydrogen-bonding network that surrounds the isoalloxazine ring in the dark and light states of AppA (dAppA and lAppA, respectively) is shown in Figure 1. Y21 and Q63 are conserved in all BLUF proteins, and replacement of these residues with residues such as F, A (Y21) and N, E, L (Q63) results in a photoinactive protein.[9−12] Although W104 is not completely conserved, in AppA changes in interactions between this residue and the hydrogen-bond network are thought to be important for photoactivation.[11] Indeed, while most W104 variants undergo the red shift in flavin spectrum, it was shown that W104A AppA is unable to function as a competent photoreceptor,[13] consistent with the inability of light excitation to modulate the β-sheet structure in this mutant,[14] and with our own studies using ultrafast time-resolved multiple probe spectroscopy.[15] In addition, W104A recovers the dark state much more rapidly than in the wild-type protein (half-life of 4 s as compared to 15 min).[14]

There are a number of mechanisms proposed for signaling state formation, which differ mainly in the roles of Y21 and Q63 in the photocycle (Figure 1). The first implicates electron transfer from Y21 to the flavin as the first step following blue light excitation, followed by rotation of Q63.[6] A second suggests that direct proton transfer from Y21 to N5 of the flavin occurs.[10] We have proposed that a photoexcitation-induced keto−enol tautomerism of the Q63 side chain precedes rotation of this residue,[9,15,16] and have also obtained data that argue against formation of a stable radical intermediate in dAppA.[17,18]

Although the photoactivation process has been intensively studied, much less is known about the mechanism of light to dark state recovery in BLUF proteins, presenting a critical gap in knowledge that must be bridged if the BLUF proteins are to be used as optogenetic tools. Hellingwerf and co-workers speculated that formation of the basic form of Y21 might be involved in stabilization of the light state, based on the observation that the rate of recovery increased ∼3-fold as the pH was increased from 8 to 11.[10] Subsequently, evidence has emerged that strongly supports proton transfer in the rate-limiting step on the reaction coordinate from the light to the dark state. This includes observations that recovery of the AppA dark state occurs with a solvent isotope effect (variously reported as either ∼2[19] or 4.7[8]) and the discovery that 2 M imidazole accelerates decay of the light state ∼100-fold.[8] A large solvent isotope effect has also been observed on the rate of dark state recovery for PixD (Slr1694),[19,20] suggesting that rate-limiting proton transfer might be a common factor in recovery of the dark state across the BLUF protein family.

To further explore the mechanism of dark state recovery, the understanding of which will have significant implications for optogenetic applications of BLUF photosensors,[20] we have introduced fluorotyrosine analogues specifically into the key residue Y21 of the AppA BLUF domain ($AppA_{BLUF}$). The fluorinated derivatives alter both the pK_a and the redox potential of the tyrosine but are expected to cause little or no perturbation to the structure.[21] This method has been used previously to study the mechanism of electron and proton transfer in numerous systems including photosystem II,[22] GFP,[23] and ribonucleotide reductase.[21,24−28] In addition, Mathes, Kennis, and co-workers have used this approach to study the photoactivation and light state decay of PixD where they observed that replacement of Y8 (the Y21 homologue in PixD) with 2-fluorotyrosine reduced the rate of recovery ∼4-fold, whereas the 3-fluorotyrosine analogue had only a small effect on the recovery rate.[29] In the present work, we observe that replacement of Y21 in $AppA_{BLUF}$ with mono-, di-, and trisubstituted fluorotyrosines, which alter the pK_a of the tyrosine in aqueous solution from 9.9 to 6.4, result in only a small change in the rate of light state formation, but dramatically accelerate the rate of dark state recovery. Specifically, the 3.5 unit reduction in pK_a results in a 4000-fold increase in the rate of recovery with a Brønsted coefficient of 1.0, indicating that the Y21 proton is completely transferred in the rate-limiting transition state on the reaction coordinate for dark state recovery. Using this information, we propose a mechanism for dark state recovery.

EXPERIMENTAL SECTION

Materials. 2-Fluorophenol, 3-fluorophenol, and 2,6-difluorophenol were purchased from Sigma-Aldrich. 2,3-Difluorophenol was purchased from Acros Organics. 2,3,6-Trifluorophenol was purchased from Oakwood Chemical. Pyridoxal-5′-phosphate, flavin adenine dinucleotide, and MEM vitamins were purchased from Sigma-Aldrich. M9 minimal media salts were from MP Biomedicals.

Tyrosine Phenol Lyase (TPL) Purification. The gene encoding tyrosine phenol lyase (TPL) was amplified by PCR from *Citrobacter freundii* (ATCC: 29063) using the primers 5′-CTAGCTAGCAT-

DOI: 10.1021/jacs.5b11115
J. Am. Chem. Soc. 2016, 138, 926−935

GAATTATCCGGCAGAACCC-3′ and 5′-CCGCTCGAGGATA-TAGTCAAAGCGTGCAGT-3′. The PCR product and pET23b expression vector were digested with *Nhe*I and *Xho*I and purified by electrophoresis (2% agarose gel). After gel extraction, the digested PCR product and pET23b vector were ligated overnight and then transformed into *E. coli* XL1-Blue cells. Colonies that grew on agar containing ampicillin (Amp) were cultured in LB-Amp media, and after the cells were harvested, the ligated plasmid was isolated using a Wizard mini-prep kit. BL21(DE3)pLysS *E. coli* cells were transformed by the resulting plasmid for protein expression. A single colony was used to inoculate 10 mL of LB media containing 0.5 mM Amp and 0.5 mM chloramphenicol (Cam), which was then incubated at 37 °C at 250 rpm overnight. This culture was then used to inoculate 1 L of LB/Amp/Cam media, in 4 L flasks, which were grown at 37 °C for ∼2.5 h until the OD_{600} reached ∼0.8. The temperature was then decreased to 25 °C for 30 min followed by addition of 0.5 mM IPTG to induce protein expression. After overnight incubation, the cells were harvested by centrifugation at 5000 rpm (4 °C) and immediately processed to ensure maximum protein yield. The cell pellet was resuspended in lysis buffer (0.1 M NaH_2PO_4, 150 mM NaCl, 5 mM imidazole, 5 mM β-mercaptoethanol, 0.1 mM pyridoxal 5′phosphate buffer at pH 7.0), and the cells were lysed using sonication (6 × 45 s at 18 W and 1 min on ice between cycles). The cell debris was removed using centrifugation (33000 rpm for 90 min), and TPL was purified using Ni-NTA chromatography (Qiagen). After the sample was loaded onto the Ni-NTA column, the column (50 mL total column volume/10 mL of resin) was washed with 0.1 M NaH_2PO_4, pH 7.0 buffer containing 150 mM NaCl and 5 mM β-mercaptoethanol, which also contained increasing amounts of imidazole (0, 10, and 20 mM), after which the protein was eluted with 5 mL fractions of the same buffer containing 250 mM imidazole. Fractions containing TPL were pooled and loaded onto a size exclusion column (Sephadex G-25), and chromatography was performed with 0.1 M NaH_2PO_4 pH 7.0 buffer containing 150 mM NaCl. Fractions containing TPL were pooled, and the purity of the protein was determined using SDS-PAGE. After concentration to ∼5 mg/mL, the purified TPL was stored at 4 °C in 20% glycerol. We found that protein could be stored under these conditions for no more than 7 days.

Fluorotyrosine Synthesis Using Tyrosine Phenol Lyase (TPL). The fluorotyrosines were synthesized from the respective fluorophenols on the basis of a method described by Stubbe and co-workers.[21] Reaction mixtures (1 L) contained 10 mM fluorophenol, 60 mM pyruvic acid, 40 μM pyridoxal-5′-phosphate, 30 mM ammonium acetate, and 5 mM β-mercaptoethanol. The pH of the reaction mixture was adjusted to 8.0 using NH_4OH, filtered using a 22 μm filter, and 160 units/L (0.53 mg = 1 unit) of purified TPL was then added. The reaction mixture was stirred in the dark at room temperature for a minimum of 4 days, and ∼30 units of fresh TPL was added every other day. Purification of the fluorotyrosines was performed by first acidifying the mixture using 5% trichloroacetic acid to precipitate out TPL. The precipitated protein was removed by centrifugation at 5000 rpm for 25 min (4 °C), or by gravity filtration, and the mixture was then extracted twice using an equal volume of ethyl acetate to remove excess phenol. The aqueous layer was heated to solubilize the product, cooled to room temperature, and loaded onto a 200 mL cation exchange Amberlite column activated with 50 mL of 2 N HCl. The column was then washed with 500 mL of distilled deionized water, and the fluorotyrosines were eluted with 250 mL of 10% NH_4OH. Fractions containing fluorotyrosine were identified using ninhydrin stain (4% ninhydrin), combined, concentrated using a rotary evaporator, lyophilized, and stored at 4 °C. This method was used to synthesize 2-fluoro-L-tyrosine (2-FY), 3-fluoro-L-tyrosine (3-FY), 2,3-difluoro-L-tyrosine (2,3-F_2Y), 3,5-difluoro-L-tyrosine (3,5-F_2Y), and 2,3,5-trifluoro-L-tyrosine (2,3,5-F_3Y). During this process, we discovered that the aqueous layer only had to be heated for purification of tyrosine because the lower pK_a enabled solubilization of the modified tyrosines at room temperature. 2-FY, 3-FY, 2,3-F_2Y, 3,5-F_2Y, and 2,3,5-F_3Y were characterized by mass spectrometry, ^{1}H NMR, and ^{19}F NMR spectroscopy (Figures S1 and S2).

Preparation of $AppA_{BLUF(Y56F)}$. Site-directed mutagenesis was used to introduce the Y56F mutation into a plasmid carrying the gene for $AppA_{BLUF}$ (residues 5−125 in pET15b vector) using primers 5′-ACC GGC GCG CTC TTC TTC AGC CAG GGC GTC TTC-3′ (forward) and 5′-GAA GAC GCC CTG GCT GAA GAA GAG CGC GCC GGT-3′ (reverse). After verifying the sequence of the construct ($AppA_{BLUF(Y56F)}$), protein expression was performed as previously described.[9] Briefly, BL21(DE3) *E. coli* cells were transformed by the $AppA_{BLUF(Y56F)}$ plasmid, and a single colony was used to inoculate a 10 mL culture of LB media containing 0.5 mM Amp. After being incubated at 37 °C and 250 rpm overnight, this culture was used to inoculate 1 L of LB/Amp media in a 4 L flask. The 4 L flask was shaken at 37 °C until the OD_{600} reached ∼0.8. Subsequently, the temperature was decreased to 18 °C followed by addition of 0.8 mM IPTG to induce protein expression overnight (16 h) in the dark.

Incorporation of 2-FY. 2-FY is recognized by the tyrosyl-tRNA synthetase and can be incorporated by simply adding this amino acid analogue to *E. coli* cells carrying the AppA plasmid and grown in minimal media. This method replaces every tyrosine in the expressed protein with 2-FY, and to incorporate 2-FY specifically into position 21, the Y56F AppA mutant ($AppA_{BLUF(Y56F)}$) was used to leave Y21 as the sole tyrosine. A single colony of BL21(DE3) *E. coli* cells carrying the $AppA_{BLUF(Y56F)}$ plasmid was streaked on agar containing M9 minimal media, glucose (2.5 mg/mL), and Amp (200 μg/mL). A colony from the M9 plate was then used to inoculate 500 mL of M9/Amp minimal media in a 4 L flask containing 5 g of sterile glucose and 5 mL of 100X MEM vitamin solution, which were added after autoclaving. The culture was shaken at 37 °C for 24 h until the OD_{600} reached ∼0.8. The cells were then harvested by centrifugation, resuspended in fresh media containing 300 mg of 2-FY, and incubated for a further 30 min at 18 °C. Subsequently, 0.8 mM IPTG was used to induce protein expression for 5 h in the dark before harvesting. The cell pellet resulting from a 1 L culture was resuspended in 40 mL of buffer A (50 mM NaH_2PO_4, 10 mM NaCl, pH 8.0) to which were added 200 μL of the protease inhibitor, phenylmethanesulphonylfluoride (50 mM stock solution in ethanol), and 14 μL of β-mercaptoethanol. The cells were then lysed using sonication, cell debris was removed by centrifugation (33000 rpm for 90 min), and the supernatant was incubated with 10 mg of FAD for 45 min on ice in the dark to ensure a homogeneous population of protein bound chromophore. Following incubation, the solution was loaded onto a Ni-NTA column (1 × 10 cm) that had been equilibrated with buffer A, and then washed with 50 mL of buffer A. The column was then washed with buffer A containing increasing concentrations of imidazole until $AppA_{BLUF(Y56F)}$ 2-FY21 eluted at 250 mM imidazole. The fractions containing protein were pooled, dialyzed against buffer A overnight, and concentrated to 1.5 mM. Protein purity was assessed by SDS-PAGE, and the chromophore content was determined from the ratio of the absorbance at 270 nm (protein and flavin) and 446 nm (flavin) (Figure S3). This ratio is 4.2 for wild-type $AppA_{BLUF}$ (ε_{270} = 35 800 M^{-1} cm^{-1}; ε_{446} = 8500 M^{-1} cm^{-1}).[30] To exchange the protein into D_2O, samples of AppA were frozen in liquid N_2, lyophilized overnight, redissolved in D_2O, and allowed to incubate for 5 h, after which this process was repeated 3−4 times. Both exchanged and unexchanged proteins were stored as lyophilized powders at 4 °C until needed. Percent incorporation of 2-fluorotyrosine was determined using a trypsin digest and MALDI mass spectrometry showing >96% incorporation (Figure S4).

Incorporation of Fluorotyrosines Using Orthogonal Aminoacyl-tRNA Synthetases. To extend our study to fluorotyrosine analogues with lower pK_a values, 3-FY, 2,3-F_2Y, 3,5-F_2Y, and 2,3,5-F_3Y were also incorporated into position 21 of $AppA_{BLUF(Y56F)}$. These analogues are not recognized by tyrosyl-tRNA synthetase, and instead were introduced into the protein using two orthogonal polyspecific aminoacyl-tRNA synthetases, E3 and E11, generously provided by Prof. Stubbe.[25] Because 2-FY was incorporated into the Y56F $AppA_{BLUF}$ mutant, this variant was also used for the other fluorotyrosine analogues. Site-directed mutagenesis was first used to convert the codon for Y21 to the amber codon (TAG) in $AppA_{BLUF(Y56F)}$ 1−125. In addition, a C-terminal 6His-tag $AppA_{BLUF(Y56F)}$ construct was used (pET20b) so that only protein with a fluorotyrosine incorporated at position 21 was able to bind to the Ni-NTA affinity purification resin. The $AppA_{BLUF(Y56F)}$ plasmid with the Y21-TAG mutation was cotransformed into BL21-

DOI: 10.1021/jacs.5b11115
J. Am. Chem. Soc. 2016, 138, 926−935

(DE3) *E. coli* cells together with either the E3 or the E11 pEVOL plasmid, and plated on LB agar containing both Amp (200 μg/mL) and Cam (50 μg/mL) to select cells harboring both plasmids. A colony from the LB/Amp/Cam plate was used to start a 10 mL overnight culture, which was subsequently used to inoculate 500 mL of 2X-YT media containing Amp and Cam. The culture was grown until the OD_{600} reached ∼0.4, and a fluorotyrosine analogue dissolved with NaOH was added to the media to give a final concentration of ∼1 mM. After 1/2 h of incubation, 0.05% w/v arabinose was added to induce expression of the E3 or E11 synthetase. The culture was incubated at 37 °C (250 rpm) until the OD_{600} reached ∼1.0, and then 0.8 mM IPTG was added to the media. After incubating overnight at 30 °C (250 rpm), the cells were harvested and purified using the same protocol as that described for the purification of $AppA_{BLUF(Y56F)}$ 2-FY21 (above).

Because a C-terminal His-tag is used, only fully translated protein can bind to the Ni-NTA resin, thus selecting against protein lacking an amino acid at position 21. Thus, as expected, MALDI analysis of tryptic peptides did not detect any native tyrosine in the fluorotyrosine-substituted proteins except for the $AppA_{BLUF(Y56F)}$ 3-FY21 where the sample contained ∼1% of the native protein. Conservatively, we estimate that the detection limit of this analytical method is 1%, and so we are confident that the fluorotyrosine content of each variant was ≥99% (Figure S5).

Time-Resolved UV−Vis Spectroscopy. Absorption spectra of each protein were obtained using an Ocean Optics USB2000+ spectrometer. This instrument collects spectra from 200 to 900 nm on the millisecond time scale using a diode array detector, with a minimum integration time of 10 ms. The white light source that was used during the recovery measurements was attenuated with a neutral density filter before it reached the sample to avoid saturating the spectrometer. In addition, it was shown that this source alone did not cause any photoconversion of the sample (Figure S6). Spectra of dark adapted $AppA_{BLUF(Y56F)}$ and the fluorotyrosine-substituted variants were first obtained, and then the sample was irradiated with ∼500 mW of 455 (±10) nm light until the photostationary state was generated. The light state spectrum was then acquired immediately after illumination was discontinued, except in the case of $AppA_{BLUF(Y56F)}$ 2,3,5-F_3Y, which recovered so rapidly that the light state spectrum had to be acquired during illumination of the sample, resulting in an artifact in the light state spectrum around 455 nm due to scattered LED light. Subsequently, spectra were recorded as a function of time during the light to dark relaxation in the absence of irradiation.

Time-Resolved and Steady-State FTIR Spectroscopy. Light minus dark FTIR spectra were obtained with 1 cm^{-1} resolution on a Vertex 80v (Bruker) FTIR spectrometer using a Harrick liquid cell equipped with CaF_2 windows and a 50 μm spacer. The light state was generated by 3 min irradiation using a 460 nm high power mounted LED (Prizmatix, Ltd.) placed in the sample compartment and focused onto the cell using an objective. The temperature of the sample holder was controlled using a circulating water bath, and data were acquired at 20 °C. The spectrometer was operated in rapid scan mode to obtain spectra of the sample as a function of time once irradiation was initiated and then discontinued. This enabled the formation of the light state to be monitored and the rate of light state decay to be directly quantified. In each case, a background spectrum of the dark adapted protein was acquired prior to initiating the photoreaction. Subsequently, light state formation was monitored by acquiring scans until the steady state was reached, and then recovery of the dark state was followed after terminating illumination. In general, scans were obtained every 200 ms. The background spectra were subtracted from the full data set, and time traces were fit to a single exponential function. The estimated rate constant for the recovery using rapid scan was determined from global analysis of the data from 1590−1710 cm^{-1}. Measured protein samples were in D_2O buffer (50 mM NaH_2PO_4, 10 mM NaCl, pD 8.0) at a concentration of ∼1−2 mM where 80 μL of sample was used for each experiment.

Ultrafast Time-Resolved Infrared Spectroscopy. Ultrafast time-resolved IR (TRIR) spectra were measured at the STFC Central Laser Facility with ∼100 fs time resolution.[31] TRIR spectra were acquired at 20 °C from 1300−1800 cm^{-1} at a resolution of 3 cm^{-1} per pixel. Data were obtained using a 50 μm path length flow cell operated at 1.5 mL/min, which was also rastered in the excitation beam to minimize photochemistry (photobleaching, photodegradation, and photoconversion). The excitation beam of the 450 nm 100 fs 5 kHz pulses was focused to a spot size of ∼100 μm, and the pulse energy was kept below 400 nJ to avoid formation of the light state. Transient difference spectra (pump on−pump off) were recorded using the IR probe at time delays between 1 ps and 2 ns. After the measurements were recorded, the extent of photoconversion was shown to be negligible using absorbance spectroscopy. Spectra were calibrated relative to the IR transmission of a pure *cis*-stilbene standard sample placed at the sample position.

Time-Resolved Multiple Probe Spectroscopy (TRMPS). TRMPS spectra were obtained at 20 °C from 100 fs to 200 μs at the STFC Central Laser Facility.[32] The TRMPS method has been described,[33] and previously used by us to analyze the photoactivation of $AppA_{BLUF}$.[15] Light-sensitive samples were analyzed using a rastered flow cell, and data were acquired using a 450 nm pump operated at 0.6−0.8 μJ per pulse and a repetition rate of 1 kHz. After the measurements were recorded, the extent of photoconversion was shown to be negligible using absorbance spectroscopy. The spectral resolution was 3 cm^{-1}, and the temporal resolution was 200 fs. A typical measurement was acquired during 45 min of data collection. All samples were prepared at 1−2 mM concentration in D_2O buffer (50 mM NaH_2PO_4, 10 mM NaCl, pD 8.0). Spectra were calibrated relative to the IR transmission of a pure *cis*-stilbene standard sample placed at the sample position. Data were analyzed globally using the sequential model with the Glotaran software package.[34]

RESULTS

Synthesis and Incorporation of Fluorotyrosine Residues. The fluorotyrosine analogues were synthesized using tyrosine phenol lyase (TPL), which catalyzes the synthesis of tyrosine from phenol, ammonia, and pyruvate.[21,25] TPL is able to accept a variety of tyrosine analogues, and this method was used to synthesize tyrosine substituted with fluorine at the 2 (2-FY), 3 (3-FY), 2,3 (2,3-F_2Y), 3,5 (3,5-F_2Y), and 2,3,5 (2,3,5-F_3Y) positions. 2-FY was incorporated into position Y21 by feeding to bacteria expressing $AppA_{BLUF(Y56F)}$, whereas the other fluorotyrosine analogues were incorporated into position 21 by amber codon mutagenesis using the E3 and E11 aminoacyl-tRNA synthetases.[25] The $AppA_{BLUF(Y56F)}$ mutant was used so that feeding experiments only introduced 2-FY into position 21. Prior to these studies, we first demonstrated that $AppA_{BLUF(Y56F)}$ had a photocycle indistinguishable from that of the wild-type protein (Figure S5), in agreement with the findings of Iwata et al.[35] All proteins contained ≥99% fluorotyrosine based on MALDI mass spectrometry (Figures S4 and S5). Following purification, each labeled protein had an absorption spectrum indistinguishable from that of dark-adapted wild-type $AppA_{BLUF}$. In addition, the absorbance spectrum of all five variants shifted to the red upon irradiation and then relaxed back to the position observed in the dark state, indicating that the proteins were photoactive. Representative data are shown in Figure 2.

Analysis of the Forward Photoreaction. As an initial step in gauging the impact of the fluorotyrosine substitutions on the photophysics of AppA, we characterized the forward photoreaction using ultrafast TRIR and time-resolved multiple probe infrared spectroscopy (TRMPS).[15] Both TRIR and TRMPS are time-resolved infrared difference techniques that report on changes in the infrared spectrum of the chromophore and protein following photoexcitation, the main difference being that TRIR covers the picosecond to nanosecond time domain, whereas TRMPS makes measurements out to 1 ms.[33] Here, the main emphasis is on the TRMPS method, which has previously been used to characterize the light-driven structural dynamics of

DOI: 10.1021/jacs.5b11115
J. Am. Chem. Soc. 2016, 138, 926−935

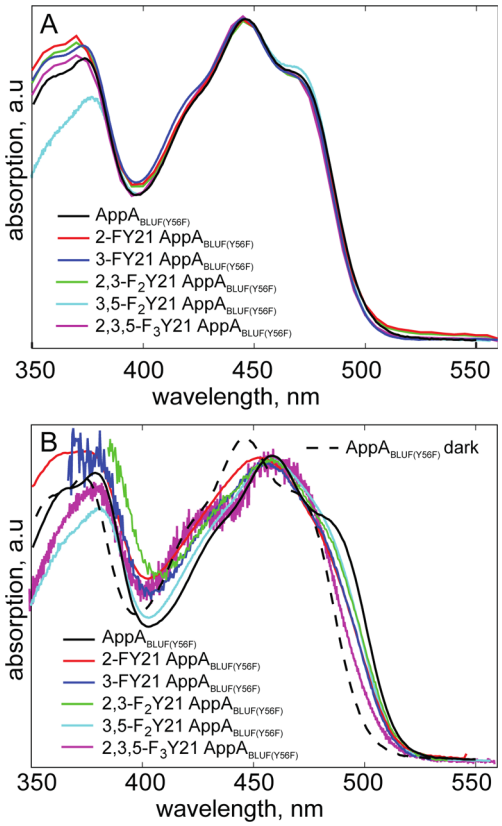

Figure 2. Absorption spectra of fluorotyrosine-substituted AppA$_{BLUF(Y56F)}$. (A) Comparison of the absorption spectra of AppA$_{BLUF(Y56F)}$, and the fluorotyrosine-substituted variants in the dark state. The dark state spectra of all of the fluorotyrosine-substituted proteins are very similar to each other and to that of AppA$_{BLUF(Y56F)}$. (B) Light adapted absorption spectra of AppA$_{BLUF(Y56F)}$, and the fluorotyrosine-substituted variants measured at the photostationary state. In each case, the flavin absorption spectrum was found to red shift relative to the dark state spectra (dashed). The extent of the red shift varied for each protein based on the different photostationary state, which in turn depends on irradiation intensity and the rate of recovery of the dark state. The trace for AppA$_{BLUF(Y56F)}$ 2,3,5-F$_3$Y21 has a lower signal:noise ratio because of the very fast light to dark recovery (see Experimental Section). Protein concentrations were ~60 μM, and the absorption spectra have been normalized.

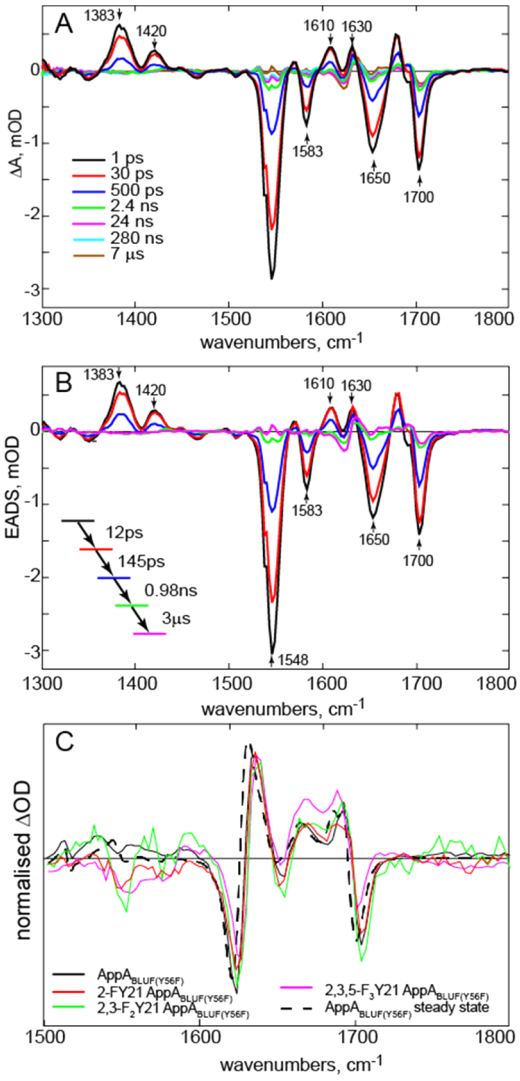

Figure 3. TRMPS and steady-state IR spectra of dAppA$_{BLUF(Y56F)}$. (A) Temporal evolution of transient IR data for AppA$_{BLUF(Y56F)}$. (B) Evolution associated difference spectra (EADS) of AppA$_{BLUF(Y56F)}$. Data were globally analyzed using the sequential model. The four time constants required (in addition to a final spectrum) to adequately describe the data were: 11 ps, 145 ps, 1 ns, and 3 μs. (C) Comparison of the spectra at 40 μs for AppA$_{BLUF(Y56F)}$ and 2-FY21, 2,3-F$_2$Y21, and 2,3,5-F$_3$Y21 AppA$_{BLUF(Y56F)}$, together with the steady-state FTIR difference spectrum of AppA$_{BLUF(Y56F)}$.

AppA$_{BLUF}$ from 100 fs to 50 μs,[15] and in general TRIR was used only to confirm the subnanosecond dynamics characterized by TRMPS. In Figure 3A, we show the time evolution of the transient IR spectrum of AppA$_{BLUF(Y56F)}$ following 450 nm excitation of the flavin (isoalloxazine) chromophore. Negative bands (bleaches) appearing at time zero are due to vibrational modes arising from photoinduced changes of the chromophore ground state, or from structural changes to the protein caused by photoexcitation. Positive bands (transients) arise from the electronic excited state of the chromophore, or from photoinduced changes in the protein modes.

The TRMPS spectrum of AppA$_{BLUF(Y56F)}$ is identical to that of wild-type AppA$_{BLUF}$ (Figure S7). Major bleaches in the spectrum that appear within the time resolution of the experiment are observed at 1700, 1650, 1583, and 1548 cm^{-1}. These bands have previously been assigned to the flavin C4=O and C2=O carbonyl groups (1700, 1650 cm^{-1}) as well as C−N vibrations of the isoalloxazine ring (1583 and 1548 cm^{-1}). In addition, several transients also appear instantaneously at 1383, 1420, 1610, 1630, and 1650 cm^{-1}. The 1383 and 1420 cm^{-1} bands are excited-state modes of the chromophore, while those at 1600 and 1630 cm^{-1} are protein modes perturbed upon excitation. As discussed previously, most of the flavin population has relaxed back to the electronic ground state by ~1 ns. This subnanosecond relaxation is adequately fit by a sum of two exponential functions (τ_1 = 0.012 and τ_2 = 0.145 ns), indicating the presence of more than one ground-state structure with different relaxation rates (Figures 3, 4; Table 1). The spectrum that remains at 1 ns and 3 μs provides an estimate of the amount of the excited state that partitions to the light state. Analysis of the high wavenumber bleaches indicates that about 5% of the intensity remains at 1 ns and 3 μs as compared to the intensity of the spectrum formed instantaneously following photoexcitation. This suggests a quantum yield for both AppA$_{BLUF(Y56F)}$ and wild-type AppA$_{BLUF}$ that is significantly lower than the value of 24% reported previously.[36]

DOI: 10.1021/jacs.5b11115
J. Am. Chem. Soc. 2016, 138, 926−935

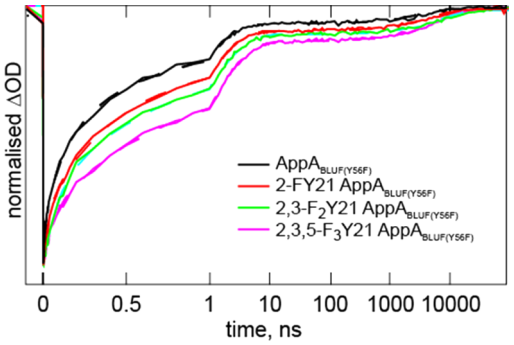

Figure 4. Ground-state recovery at 1548 cm^{-1} from the TRMPS data. Dashed lines are the results of global analysis, and the solid lines are the raw data. The first nanosecond of the data are plotted on a linear scale, while the remainder is plotted on a logarithmic scale. The time constants for each protein are given in Table 1.

Table 1. Spectral Evolution from the TRMPS Data[a]

	τ_1/ns	τ_2/ns	τ_3/ns	τ_4/ns
AppA$_{BLUF(Y56F)}$	0.012	0.145	1.0	3000
2-FY21 AppA$_{BLUF(Y56F)}$	0.03	0.33	1.5	4850
3-FY21 AppA$_{BLUF(Y56F)}$	0.016	0.42	2.6	4150
2,3-F$_2$Y21 AppA$_{BLUF(Y56F)}$	0.08	0.54	2.4	7200
2,3,5-F$_2$Y21 AppA$_{BLUF(Y56F)}$	0.065	0.6	2.7	8200

[a]Data were globally analyzed using Glotaran,[34] and in each case four time constants plus the final spectrum were required to adequately describe the data.

The subsequent evolution of the spectrum remaining after 1 ns results from the structural dynamics in the protein leading to the final ground-state photoactivated protein (lAppA). This evolution from 1 ns to ∼20 μs can again be adequately described by two exponential functions with time constants of 1 (τ_3) and 3000 (τ_4) ns (Figures 3, 4; Table 1). Evidence that the spectral evolution is complete by 40 μs is shown by the similarity between the TRMPS difference spectrum at 40 μs for each protein and the corresponding steady-state FTIR difference spectrum of AppA$_{BLUF(Y56F)}$ (Figure 3C). No further evolution of the TRMPS spectra is observed up to 200 μs, which is the longest time point analyzed (Figure S8).

The TRMPS data for AppA$_{BLUF(Y56F)}$ are compared to the corresponding spectra of the fluorotyrosine-substituted proteins (Figure S9). The corresponding rate constants for spectral evolution obtained from the global analysis are given in Table 1. Two conclusions can be drawn from the data. First, the positions and amplitudes of the major bleaches and transients for each fluorotyrosine protein closely match those of AppA$_{BLUF(Y56F)}$, suggesting that the incorporation of the unnatural amino acids has not had a significant effect on the protein structure and its interactions with the chromophore. Second, in each case, spectral evolution can be adequately described by four rate constants, two for the initial subnanosecond ground-state recovery, and two for the subsequent formation of the final photoactivated ground state. Thus, the inhomogeneity observed in wild-type AppA$_{BLUF}$ as well as AppA$_{BLUF(Y56F)}$ is also present for the fluorotyrosine mutants (Figures S7 and S9).

Table 1 reveals a small effect resulting from alteration in the pK_a and reduction potential of residue 21: as the pK_a decreases by ∼3.5 units from Y21 to 2,3,5-F$_3$Y21 and the reduction potential E_p(Y$^{\bullet}$/Y^{-}) increases by ∼200 mV,[21] each time constant increases by a factor of ∼3. Thus, the 3200-fold increase in acidity of Y21 has resulted in a small (<3-fold) decrease in both the rate of the initial ground-state recovery and the rate of formation of the final photoactivated ground state. The observation that both the subnanosecond (excited electronic state) and the microsecond (ground electronic state) data change by similar factors, as the pK_a and E_p values of residue 21 are altered, is significant. Specifically, it does not support a mechanism that involves electron transfer in AppA, as the subnanosecond kinetics would be expected to be more sensitive to the reduction potential of Y21 than the microsecond kinetics, when the fully oxidized flavin is in its electronic ground state. This is consistent with a previous discussion on the effect of 2-FY21 and 3-FY21 on the primary step in the AppA photocycle.[17]

Dark State Recovery. Recovery of the AppA$_{BLUF}$ dark state was monitored using both absorption spectroscopy and rapid scan FTIR spectroscopy. Formation of the light state results in a red shift in the 450 nm flavin spectrum, and the rate of dark state recovery was measured by following the relaxation of the red-shifted spectrum using a spectrometer with a 1 ms time resolution (Figures 2 and 5). The recovery rate was measured in both H$_2$O and D$_2$O buffer (Table 2), and as a function of pH, by fitting the absorbance change measured at 480−510 nm to a single exponential equation (Table S1). We also used difference FTIR spectroscopy to monitor relaxation of the dark state for two representative variants, AppA$_{BLUF(Y56F)}$ and AppA$_{BLUF(Y56F)}$ 2,3-F$_2$Y21. In both cases, there was good correspondence between the rates obtained from FTIR with those determined from the UV−vis absorption spectra (Figure 5D). This indicates that the change in the electronic spectrum of the flavin and alteration in the protein structure observed by FTIR are reporting on the same structural change in the protein. A representative series of FTIR difference spectra for AppA$_{BLUF(Y56F)}$ 2,3-F$_2$Y21 obtained using the rapid scan mode are shown in Figure S10. Variation of the pH had only a small impact on the rate of dark state recovery (Table S1), as reported previously for wild-type AppA$_{BLUF}$.[10] However, while modulation in the pK_a of residue 21 had little effect on the forward reaction, the rate of dark state recovery in H$_2$O increased 4000-fold as the pK_a decreased from 9.9 (Y21) to 6.4 (2,3,5-F$_3$Y21). A plot of pK_a against the log of the first-order rate constant yielded a straight line (R = 0.99) with a slope of ∼1.0 (Figure 6), consistent with a rate-limiting proton transfer in the mechanism of dark state recovery. The Brønsted coefficient of 1.0 indicates that the proton is completely transferred in the rate-limiting transition state.

The Brønsted plot in D$_2$O was also linear with a slope of 1.09. The observation of a solvent isotope effect (SIE) on dark state recovery is consistent with previous reports for AppA (SIE 2−4.7)[8,19] and PixD (SIE 4),[37,38] supporting the importance of proton transfer in this step. The data in Table 2 also reveal a significant solvent isotope effect for dark state recovery that ranges from 5 for AppA$_{BLUF(Y56F)}$ to almost 9 for 3-FY21 and to 2.3 for 2,3,5-F$_3$Y21.

DISCUSSION

All BLUF-containing photoreceptors so far characterized operate through light-driven formation of the photoactive state followed by recovery of the dark state through a light-independent reaction. Formation of the light state occurs rapidly and is complete within a few tens of microseconds. Various mechanisms have been proposed for the forward reaction, and for the best characterized BLUF protein AppA our data support a model in which the initial event involves light-induced keto−enol tautomerism of a conserved glutamine (Q63) leading ultimately

DOI: 10.1021/jacs.5b11115
J. Am. Chem. Soc. 2016, 138, 926−935

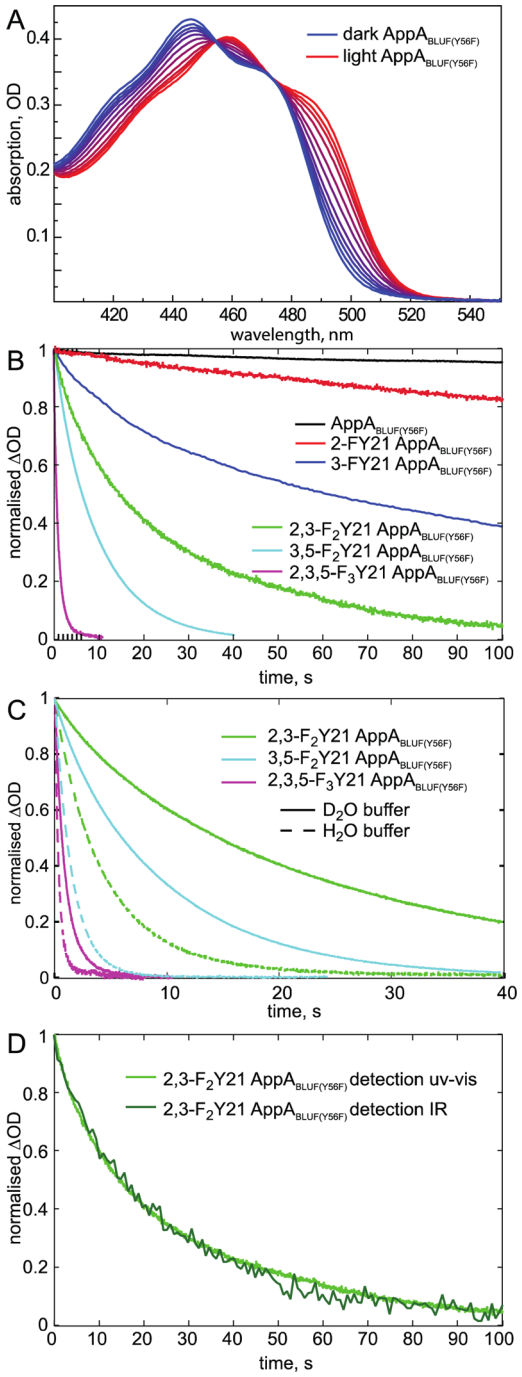

Figure 5. Dark state recovery kinetics. Dark state recovery kinetics were obtained by monitoring the visible absorption spectrum of AppA. (A) Spectral evolution of AppA$_{BLUF(Y56F)}$, following irradiation at 455 nm. (B) Recovery kinetics in D_2O buffer. (C) Comparison of the recovery kinetics in H_2O and D_2O buffer for selected proteins. (D) Comparison of the recovery kinetics of AppA$_{BLUF(Y56F)}$ 2,3-F_2Y21 in D_2O obtained by monitoring time-dependent changes in the electronic absorption spectrum (estimated recovery rate 0.04 s^{-1}) or the FTIR spectrum at 1686 cm^{-1} (estimated recovery rate 0.038 s^{-1}). In each case, time constants for the recovery kinetics were obtained by fitting the data to a single exponential function. The protein concentration was ~60 μM for the UV−vis absorption measurements or ~1.5 mM for the FTIR difference spectra measurements.

to an alteration in the hydrogen-bonding network that surrounds the flavin chromophore. In contrast to the rapid light-driven photoactivation, recovery of the dark state occurs through a light-independent pathway with a half-life of seconds to minutes depending on the specific BLUF protein. For AppA, dark state recovery occurs with a half-life of about 15 min. Previous studies on dark state recovery have provided evidence for rate-limiting proton transfer through the observation of solvent isotope effects for AppA and PixD. However, little else is known about the mechanism of dark state recovery.

In the present work, we have replaced Y21 with a series of mono-, di-, and trisubstituted fluorotyrosines that range in pK_a from 9.9 (Y21) to 6.4 (2,3,5-F_3Y21). These experiments were performed in the AppA$_{BLUF(Y56F)}$ background so that only Y21 was replaced in the one variant (2-FY) that could not be produced via amber codon mutagenesis. The similarities in the vibrational peak positions from the time-resolved (TRMPS) and steady-state IR difference spectra obtained for the different variants suggest that the fluorine substituents do not significantly perturb the overall environment of the flavin or the protein structure. The forward photoreaction was examined using TRMPS and revealed a ~3-fold increase in the time constants that characterize spectral evolution over ~7 decades in time (1 ps to 20 μs). Thus, the ~3200-fold change in tyrosine acidity and 200 mV change in reduction potential have only a ~3-fold impact on the rate of light state formation, suggesting that proton or electron transfer to or from the hydroxyl group of this residue does not play a significant role in the rate-determining step(s) that lead to formation of the signaling state of the protein.

In contrast to the forward reaction, the rate of dark state recovery exhibits a very strong dependence on acidity of the Y21 hydroxyl group. Specifically, the increase in Y21 acidity through the fluorotyrosine series correlates with a 4000-fold increase in the rate of recovery in H_2O and 8800-fold increase in the rate in D_2O. This correlation is well described by a linear free energy relationship with a Brønsted coefficient of 1.0, indicating a direct connection between Y21 acidity and the mechanism of dark state recovery (Figure 6). In addition, the Brønsted coefficient of 1 indicates complete proton transfer in the rate-limiting transition state on the reaction coordinate leading from light to dark AppA$_{BLUF}$.

The above data allow us to propose a detailed mechanism for the light to dark state recovery of wild-type AppA (Figure 7) where proton transfer from Y21 to Q63 is hypothesized to be the rate-determining step in the recovery. In formulating this model, we assume that the Q63 side chain has rotated during formation of the light state[6,12] and that, like the photoactivation mechanism (Figure 1), the recovery mechanism also involves keto−enol tautomerism. In addition, although several theoretical studies[39−42] support our original proposal[9] for Q63 keto−enol tautomerism occurring during photoactivation, in the model proposed here we assume that final ground-state structures in both dark and light-adapted AppA is the more stable keto tautomer. In the light state, keto tautomer (i) (lAppA$_{keto}$) Y21 is hydrogen bonded to the Q63 carbonyl group, consistent with NMR data that show the presence of a well-defined hydrogen bond between Y21 and a neighboring residue.[43] In the rate-determining step, we suggest that Y21 protonates Q63 leading to formation of the Q63 enol. This is envisaged in Figure 7 as proton transfer to the enolate resonance form of the Q63 side chain (ii). After formation of the enol (iv), Q63 rotates, breaking the hydrogen bond to the C4═O of the flavin, and forming a new hydrogen bond with the flavin N5 atom (v). The last step involves a second tautomerization to return to the more stable keto state of Q63 (vi). In our mechanism, we assign (iv) to

DOI: 10.1021/jacs.5b11115
J. Am. Chem. Soc. 2016, 138, 926−935

Table 2. Dark State Recovery Rate Constants[a]

	pK_a	k_{H2O}/s^{-1}	k_{D2O}/s^{-1}	solvent isotope effect
$AppA_{BLUF(Y6F)}$	9.9	0.00065 ± 0.00006	0.00013 ± 0.00001	5.0 ± 1
2-FY21 $AppA_{BLUF(Y6F)}$	9.0	0.011 ± 0.001	0.0018 ± 0.0002	6.2 ± 1.2
3-FY21 $AppA_{BLUF(Y6F)}$	8.4	0.034 ± 0.002	0.0039 ± 0.0001	8.8 ± 0.7
2,3-F_2Y21 $AppA_{BLUF(Y6F)}$	7.8	0.22 ± 0.01	0.040 ± 0.001	5.5 ± 0.2
3,5-F_2Y21 $AppA_{BLUF(Y6F)}$	7.2	0.63 ± 0.02	0.11 ± 0.01	5.8 ± 0.3
2,3,5-F_3Y21 $AppA_{BLUF(Y6F)}$	6.4	2.6 ± 0.1	1.15 ± 0.03	2.2 ± 0.1

[a]Recovery rate constants were obtained from the change in absorption spectra once irradiation at 455 nm had been terminated by fitting the data to a single exponential function. Errors are based on measurements made in triplicate or quadruplicate. Recovery rates were also measured in D_2O for the $AppA_{BLUF(Y6F)}$ and $AppA_{BLUF(Y6F)}$ 2,3-F_2Y21 using fast scan FTIR. The rate constants obtained from fitting of the FTIR data were 0.00015 and 0.038, respectively, which agrees within experimental error to those measured by monitoring the change in the electronic spectrum of the flavin.

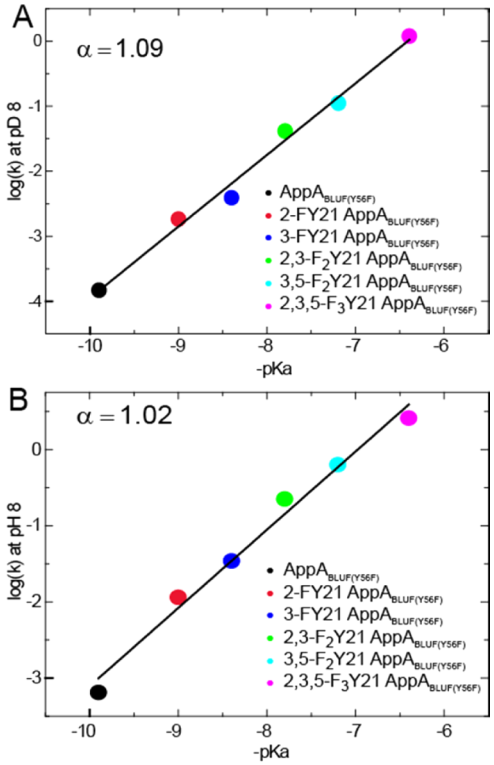

Figure 6. Brønsted plots in H_2O and D_2O. Recovery rate constants (log k) for the $AppA_{BLUF(Y6F)}$ variants plotted against the corresponding −pK_a values for tyrosine and the fluorotyrosines. Data have been fit to a linear function. (A) Data obtained in D_2O (pD 8.0). (B) Data obtained in H_2O (pH 8.0).

$lAppA_{enol}$ and (v) to $dAppA_{enol}$, although we do not know at what stage the protein structure will relax back to that found in the dark state. In (v) Y21 will now be solvent accessible and thus able to abstract a proton from the solvent. Abstraction of the proton from Y21 by Q63 (ii−iv) is the rate-determining step of the light to dark recovery, consistent with the isotope effect observed for recovery in deuterated buffer. In addition, the Brønsted coefficient of 1 indicates that proton transfer is complete in the rate-limiting transition state (iii). This mechanism also enables us to envisage a role for a base such as imidazole, which has been shown to accelerate the rate of dark state recovery.[8] For instance, general base catalysis could assist in the formation of the enol species (iv) by abstracting a proton from the Q63 NH_2 group.

While the mechanism in Figure 7 rationalizes the essential role that Y21 plays in the AppA photocycle, it also provides a basis for discussing the impact of W104 on light to dark state recovery. Although W104 is critical for coupling the change in the hydrogen-bonding network around the flavin to the alteration in protein structure that accompanies photoactivation, the exact position of W104 in the dark and light states is controversial (see Collette et al.[42] for a thorough review on the subject). However, the observation that the W104A mutant recovers ∼150-fold faster than wild-type AppA[14] suggests that W104 interacts with Q63 to either stabilize the keto form of lAppA (i) and/or destabilize the rate-limiting transition state (iii) involved in the proton transfer step. This would suggest that W104 is close to Q63 in the light state, potentially arguing against large-scale motion of W104 during photoactivation such that W104 occupies a Trp_{in} conformation in both dark and light states, or that W104 is in the "out" configuration in the dark state and in the "in" configuration in the light state.

Finally, we can return to the solvent isotope effect on dark state recovery. Apart from 2,3,5-F_3Y $AppA_{BLUF(Y6F)}$, the solvent isotope effect ranges from ∼5−9, which is unusually large for a single proton transfer step. However, conversion of the light state to the dark state must be coupled to an alteration in the conformation of the protein, because only dark adapted AppA is able to bind the transcriptional repressor PpsR, and in this regard we note that large solvent isotope effects have been reported for protein conformational changes.[44]

The present studies have focused on the BLUF domain of AppA, and one important extension of this work will be to explore how variation in tyrosine pK_a modulates the forward and reverse reactions in the context of full-length AppA and the AppA:$PpsR_2$ complex. In parallel, additional experiments will seek to determine whether the mechanism proposed here for $AppA_{BLUF}$ translates to other BLUF proteins. Solvent isotope effects are also observed on the rate of dark state recovery for the BLUF proteins PixD (4)[37,38] and BlrB (2.5),[45] indicating that proton transfer is also involved in these proteins. However, the effect of tyrosine pK_a on the rate of dark state formation has been studied for PixD where it was observed that increasing acidity decreased rather than increased the rate of recovery.[29] In addition, FTIR spectroscopy has provided evidence that Y8 in PixD from *Thermosynechococcus elongates* is protonated in both the dark and the light states.[46] Thus, significant differences may exist in the mechanism of dark state recovery throughout the BLUF domain family.

SUMMARY

We have used unnatural amino acid incorporation to probe the mechanism of photoactivation and ground-state recovery in AppA. The vibrational spectra recorded in TRMPS demonstrate that replacement of Y21 with fluorotyrosine analogues neither causes a structural perturbation in the environment of the flavin chromophore nor greatly modifies the forward photokinetics.

DOI: 10.1021/jacs.5b11115
J. Am. Chem. Soc. 2016, 138, 926−935

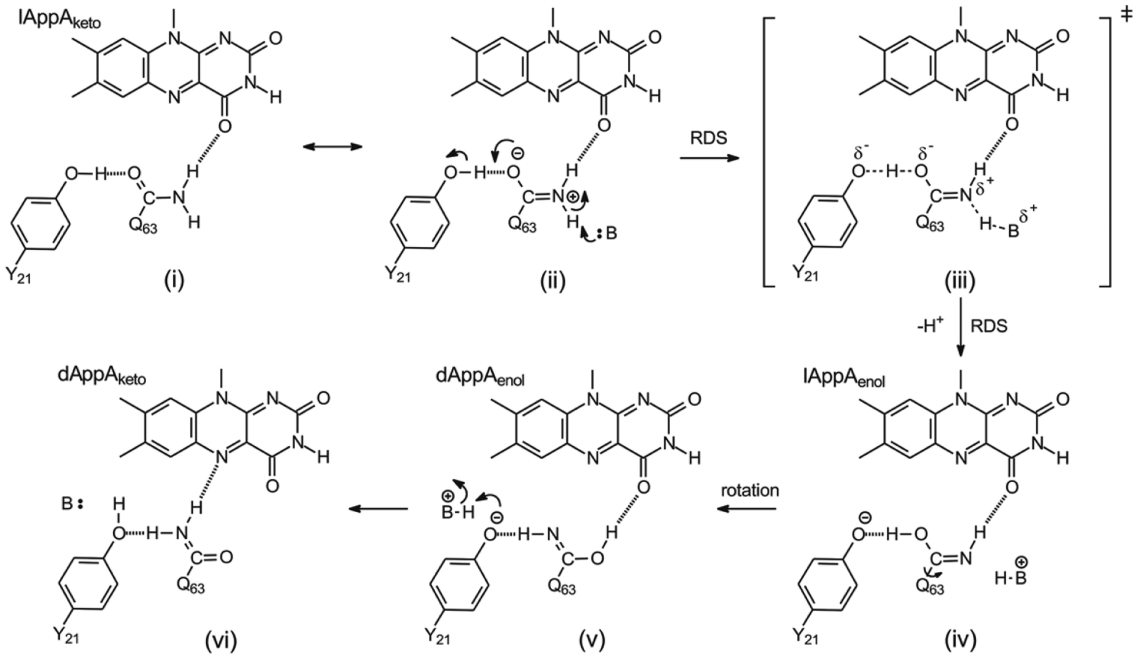

Figure 7. Mechanism of light to dark state recovery in AppA$_{BLUF}$. In the ground state of lAppA$_{BLUF}$, the Q63 side chain exists as a mixture of keto (i) and enol (ii) resonance structures.[16] Consistent with NMR solution studies,[43] this state is characterized by a hydrogen bond between Y21 and the Q63 side-chain amide carbonyl that is essential for stabilization of lAppA$_{BLUF}$. We propose that the rate-determining step (RDS) for recovery of the dark state involves proton transfer from Y21 to Q63 leading to formation of the enol form of Q63 in which the Q63 hydroxyl group is hydrogen bonded to the Y21 anion (iv). The Brønsted coefficient of 1 indicates that this proton transfer is almost complete in the rate-determining transition state (iii). During the conversion of (ii) to (iv), the Q63 amide must also lose a proton. Under normal conditions, this proton may be transferred directly to solvent; however, in our mechanism, we show a base B abstracting the proton indicating one potential way in which imidazole could act as a general base to catalyze the reaction.[8] The enol tautomer (iv) then rotates (v) and returns to the more stable keto form (vi), breaking the hydrogen bond with the C4═O of the flavin and forming a new hydrogen bond with the N5 atom of the flavin. In this mechanism, we show protonation of Y21 in the final dAppA$_{BLUF}$ species, although the pK_a of this residue is likely around 8 in the dark state. State v is labeled as dAppA$_{enol}$, although we do not know at what stage the overall protein structure relaxes from that found in lAppA to that in dAppA.

Modulation of the Y21 pK_a does, however, have a dramatic effect on the rate of light to dark state recovery following AppA photoactivation, where an increase in Y21 acidity is found to correlate with an increase in the recovery rate. A Brønsted analysis of the data indicates that the Y21 proton is completely transferred in the transition state leading from the light to the dark state. Rate-limiting proton transfer is consistent with the solvent isotope effect reported previously and has been incorporated into a mechanism for AppA recovery that involves tautomerization of residue Q63. This light to dark ground-state recovery mechanism, which highlights the importance of Y21 in the photocycle, has not been elucidated previously. The ability to control the light to dark recovery rate may have great importance in optogenetic applications of the BLUF photosensors, because the delay in recovery and/or lifetime of the signaling state could directly influence the magnitude and duration of downstream biological events triggered by photoactivation.[47,48]

■ ASSOCIATED CONTENT

Supporting Information

The Supporting Information is available free of charge on the ACS Publications website at DOI: 10.1021/jacs.5b11115.

Analytical data (MS, ^{1}H NMR, and ^{19}F NMR) for the synthesized fluorotyrosines, 2-FY, 3-FY, 2,3-F$_2$Y, 3,5-F$_2$Y, and 2,3,5-F$_3$Y, mass spectrometry data for fluorotyrosine incorporation into AppA$_{BLUF(Y56F)}$, UV−vis spectra used for calculating the chromophore content in the AppA$_{BLUF}$ proteins, a control UV−vis spectrum for the Ocean Optics instrument, additional TRMPS data sets, representative rapid scan FTIR spectra, and rate constants for dark state recovery as a function of pH (PDF)

■ AUTHOR INFORMATION

Corresponding Authors

*s.meech@uea.ac.uk

*peter.tonge@stonybrook.edu

Author Contributions

#A.A.G. and A.H. contributed equally to this work.

Notes

The authors declare no competing financial interest.

■ ACKNOWLEDGMENTS

This work was funded by the EPSRC (EP/K000764 to S.R.M.) and NSF (CHE-1223819 to P.J.T). We are grateful to STFC for access to the ULTRA laser facility. We are grateful to Professor Ray Owens and Anil Verma for assistance in protein preparation and access to the Oxford Protein Production Facility − UK. We gratefully acknowledge Professor JoAnne Stubbe for the gifts of the orthogonal aminoacyl-tRNA synthetases. J.I. was supported by an NIH Chemistry-Biology Interface training grant (T32GM092714).

■ REFERENCES

(1) Gomelsky, M.; Klug, G. *Trends Biochem. Sci.* **2002**, *27*, 497.

DOI: 10.1021/jacs.5b11115
J. Am. Chem. Soc. 2016, 138, 926−935

(2) Okajima, K.; Yoshihara, S.; Fukushima, Y.; Geng, X.; Katayama, M.; Higashi, S.; Watanabe, M.; Sato, S.; Tabata, S.; Shibata, Y.; Itoh, S.; Ikeuchi, M. *J. Biochem.* **2005**, *137*, 741.
(3) Zirak, P.; Penzkofer, A.; Schiereis, T.; Hegemann, P.; Jung, A.; Schlichting, I. *J. Photochem. Photobiol., B* **2006**, *83*, 180.
(4) Rajagopal, S.; Key, J. M.; Purcell, E. B.; Boerema, D. J.; Moffat, K. *Photochem. Photobiol.* **2004**, *80*, 542.
(5) van der Horst, M. A.; Hellingwerf, K. J. *Acc. Chem. Res.* **2004**, *37*, 13.
(6) Anderson, S.; Dragnea, V.; Masuda, S.; Ybe, J.; Moffat, K.; Bauer, C. *Biochemistry* **2005**, *44*, 7998.
(7) Masuda, S.; Bauer, C. E. *Cell* **2002**, *110*, 613.
(8) Laan, W.; Gauden, M.; Yeremenko, S.; van Grondelle, R.; Kennis, J. T.; Hellingwerf, K. J. *Biochemistry* **2006**, *45*, 51.
(9) Stelling, A. L.; Ronayne, K. L.; Nappa, J.; Tonge, P. J.; Meech, S. R. *J. Am. Chem. Soc.* **2007**, *129*, 15556.
(10) Laan, W.; van der Horst, M. A.; van Stokkum, I. H.; Hellingwerf, K. J. *Photochem. Photobiol.* **2003**, *78*, 290.
(11) Gauden, M.; Grinstead, J. S.; Laan, W.; van Stokkum, I. H.; Avila-Perez, M.; Toh, K. C.; Boelens, R.; Kaptein, R.; van Grondelle, R.; Hellingwerf, K. J.; Kennis, J. T. *Biochemistry* **2007**, *46*, 7405.
(12) Jung, A.; Reinstein, J.; Domratcheva, T.; Shoeman, R. L.; Schlichting, I. *J. Mol. Biol.* **2006**, *362*, 717.
(13) Masuda, S.; Tomida, Y.; Ohta, H.; Takamiya, K. *J. Mol. Biol.* **2007**, *368*, 1223.
(14) Masuda, S.; Hasegawa, K.; Ono, T. A. *Plant Cell Physiol.* **2005**, *46*, 1894.
(15) Brust, R.; Lukacs, A.; Haigney, A.; Addison, K.; Gil, A.; Towrie, M.; Clark, I. P.; Greetham, G. M.; Tonge, P. J.; Meech, S. R. *J. Am. Chem. Soc.* **2013**, *135*, 16168.
(16) Lukacs, A.; Haigney, A.; Brust, R.; Zhao, R. K.; Stelling, A. L.; Clark, I. P.; Towrie, M.; Greetham, G. M.; Meech, S. R.; Tonge, P. J. *J. Am. Chem. Soc.* **2011**, *133*, 16893.
(17) Lukacs, A.; Brust, R.; Haigney, A.; Laptenok, S. P.; Addison, K.; Gil, A.; Towrie, M.; Greetham, G. M.; Tonge, P. J.; Meech, S. R. *J. Am. Chem. Soc.* **2014**, *136*, 4605.
(18) Laptenok, S. P.; Lukacs, A.; Brust, R.; Haigney, A.; Gil, A.; Towrie, M.; Greetham, G. M.; Tonge, P. J.; Meech, S. R. *Faraday Discuss.* **2015**, *177*, 293.
(19) Masuda, S.; Hasegawa, K.; Ono, T. A. *Biochemistry* **2005**, *44*, 1215.
(20) Stierl, M.; Stumpf, P.; Udwari, D.; Gueta, R.; Hagedorn, R.; Losi, A.; Gartner, W.; Petereit, L.; Efetova, M.; Schwarzel, M.; Oertner, T. G.; Nagel, G.; Hegemann, P. *J. Biol. Chem.* **2011**, *286*, 1181.
(21) Seyedsayamdost, M. R.; Reece, S. Y.; Nocera, D. G.; Stubbe, J. *J. Am. Chem. Soc.* **2006**, *128*, 1569.
(22) Rappaport, F.; Boussac, A.; Force, D. A.; Peloquin, J.; Brynda, M.; Sugiura, M.; Un, S.; Britt, R. D.; Diner, B. A. *J. Am. Chem. Soc.* **2009**, *131*, 4425.
(23) Ayyadurai, N.; Prabhu, N. S.; Deepankumar, K.; Kim, A.; Lee, S. G.; Yun, H. *Biotechnol. Lett.* **2011**, *33*, 2201.
(24) Seyedsayamdost, M. R.; Yee, C. S.; Stubbe, J. *Nat. Protoc.* **2007**, *2*, 1225.
(25) Minnihan, E. C.; Young, D. D.; Schultz, P. G.; Stubbe, J. *J. Am. Chem. Soc.* **2011**, *133*, 15942.
(26) Reece, S. Y.; Seyedsayamdost, M. R.; Stubbe, J.; Nocera, D. G. *J. Am. Chem. Soc.* **2006**, *128*, 13654.
(27) Bonin, J.; Costentin, C.; Robert, M.; Saveant, J. M.; Tard, C. *Acc. Chem. Res.* **2012**, *45*, 372.
(28) Reece, S. Y.; Hodgkiss, J. M.; Stubbe, J.; Nocera, D. G. *Philos. Trans. R. Soc., B* **2006**, *361*, 1351.
(29) Mathes, T.; van Stokkum, I. H.; Stierl, M.; Kennis, J. T. *J. Biol. Chem.* **2012**, *287*, 31725.
(30) Laan, W.; Bednarz, T.; Heberle, J.; Hellingwerf, K. J. *Photochem. Photobiol. Sci.* **2004**, *3*, 1011.
(31) Greetham, G. M.; Burgos, P.; Cao, Q.; Clark, I. P.; Codd, P. S.; Farrow, R. C.; George, M. W.; Kogimtzis, M.; Matousek, P.; Parker, A. W.; Pollard, M. R.; Robinson, D. A.; Xin, Z. J.; Towrie, M. *Appl. Spectrosc.* **2010**, *64*, 1311.
(32) Greetham, G. M.; Burgos, P.; Cao, Q.; Clark, I. P.; Codd, P. S.; Farrow, R. C.; George, M. W.; Kogimtzis, M.; Matousek, P.; Parker, A. W.; Pollard, M. R.; Robinson, D. A.; Xin, Z.-J.; Towrie, M. *Appl. Spectrosc.* **2010**, *64*, 1311.
(33) Greetham, G. M.; Sole, D.; Clark, I. P.; Parker, A. W.; Pollard, M. R.; Towrie, M. *Rev. Sci. Instrum.* **2012**, *83*, 103107.
(34) Snellenburg, J. J.; Laptenok, S. P.; Seger, R.; Mullen, K. M.; van Stokkum, I. H. M. *J. Stat Softw* **2012**, *49*, 1.
(35) Iwata, T.; Watanabe, A.; Iseki, M.; Watanabe, M.; Kandori, H. *J. Phys. Chem. Lett.* **2011**, *2*, 1015.
(36) Gauden, M.; Yeremenko, S.; Laan, W.; van Stokkum, I. H.; Ihalainen, J. A.; van Grondelle, R.; Hellingwerf, K. J.; Kennis, J. T. *Biochemistry* **2005**, *44*, 3653.
(37) Masuda, S.; Hasegawa, K.; Ishii, A.; Ono, T. A. *Biochemistry* **2004**, *43*, 5304.
(38) Hasegawa, K.; Masuda, S.; Ono, T. A. *Plant Cell Physiol* **2005**, *46*, 136.
(39) Sadeghian, K.; Bocola, M.; Schutz, M. *J. Am. Chem. Soc.* **2008**, *130*, 12501.
(40) Domratcheva, T.; Grigorenko, B. L.; Schlichting, I.; Nemukhin, A. V. *Biophys. J.* **2008**, *94*, 3872.
(41) Udvarhelyi, A.; Domratcheva, T. *J. Phys. Chem. B* **2013**, *117*, 2888.
(42) Collette, F.; Renger, T.; Schmidt Am Busch, M. *J. Phys. Chem. B* **2014**, *118*, 11109.
(43) Grinstead, J. S.; Avila-Perez, M.; Hellingwerf, K. J.; Boelens, R.; Kaptein, R. *J. Am. Chem. Soc.* **2006**, *128*, 15066.
(44) Wang, M. S.; Gandour, R. D.; Rodgers, J.; Haslam, J. L.; Schowen, R. L. *Bioorg. Chem.* **1975**, *4*, 392.
(45) Wu, Q.; Ko, W. H.; Gardner, K. H. *Biochemistry* **2008**, *47*, 10271.
(46) Takahashi, R.; Okajima, K.; Suzuki, H.; Nakamura, H.; Ikeuchi, M.; Noguchi, T. *Biochemistry* **2007**, *46*, 6459.
(47) Bacchus, W.; Fussenegger, M. *Curr. Opin. Biotechnol.* **2012**, *23*, 695.
(48) Christie, J. M.; Gawthorne, J.; Young, G.; Fraser, N. J.; Roe, A. J. *Mol. Plant* **2012**, *5*, 533.

DOI: 10.1021/jacs.5b11115
J. Am. Chem. Soc. 2016, 138, 926−935